Received: 6 June 2022 | Revised: 28 September 2022 | Accepted: 12 October 2022

DOI: 10.1111/cas.15615

Cancer Science WILEY

ORIGINAL ARTICLE

Identification of a novel target of SETD1A histone methyltransferase and the clinical significance in pancreatic cancer

Takeshi Ishii[1,2] | Yoshimitsu Akiyama[1] | Shu Shimada[1] | Ayano Kabashima[1] | Daisuke Asano[2] | Shuichi Watanabe[2] | Yoshiya Ishikawa[2] | Hiroki Ueda[2] | Keiichi Akahoshi[2] | Kosuke Ogawa[2] | Hiroaki Ono[2] | Atsushi Kudo[2] | Minoru Tanabe[2] | Shinji Tanaka[1,2]

[1]Department of Molecular Oncology, Graduate School of Medicine, Tokyo Medical and Dental University, Tokyo, Japan

[2]Department of Hepato-Biliary-Pancreatic Surgery, Graduate School of Medicine, Tokyo Medical and Dental University, Tokyo, Japan

Correspondence
Yoshimitsu Akiyama and Shinji Tanaka, Department of Molecular Oncology, Graduate School of Medicine, Tokyo Medical and Dental University, 1-5-45 Yushima, Bunkyo-ku, Tokyo 113-8519, Japan.
Emails: yakiyama.monc@tmd.ac.jp and tanaka.monc@tmd.ac.jp

Funding information
Japan Agency for Medical Research and Development, Grant/Award Number: JP19cm0106540; Ministry of Education, Culture, Sports, Science and Technology, Grant/Award Number: 19H01055, 20H03526 and 20K21627; Princess Takamatsu Cancer Research Fund

Abstract

Although histone H3K4 methyltransferase SETD1A is overexpressed in various cancer types, the molecular mechanism underlying its overexpression and its target genes in pancreatic ductal adenocarcinoma (PDAC) remain unclarified. We conducted immunohistochemical staining for SETD1A in 105 human PDAC specimens to assess the relationship between SETD1A overexpression and clinicopathological features. The function and target genes of SETD1A were investigated using human pancreatic cancer cell lines. SETD1A expression was upregulated in 51.4% of patients with PDAC and was an independent prognostic factor associated with shorter disease-free survival after resection ($p < 0.05$). Knockdown and overexpression of *SETD1A* showed that SETD1A plays a crucial role in increasing the proliferation and motility of PDAC cells. *SETD1A* overexpression increased tumorigenicity. RNA sequencing of *SETD1A*-knockdown cells revealed downregulation of *RUVBL1*, an oncogenic protein ATP-dependent DNA helicase gene. ChIP analysis revealed that SETD1A binds to the *RUVBL1* promoter region, resulting in increased H3K4me3 levels. Knockdown of *RUVBL1* showed inhibition of cell proliferation, migration, and invasion of PDAC cells, which are similar biological effects to *SETD1A* knockdown. High expression of both SETD1A and RUVBL1 was an independent prognostic factor not only for disease-free survival but also for overall survival ($p < 0.05$). In conclusion, we identified *RUVBL1* as a novel downstream target gene of the SETD1A-H3K4me3 pathway. Co-expression of SETD1A and RUVBL1 is an important factor for predicting the prognosis of patients with PDAC.

KEYWORDS
histone modification, pancreatic cancer, prognostic factor, RUVBL1, SETD1A

Abbreviations: ChIP, chromatin immunoprecipitation; DFS, disease-free survival; H3K9me3, H3K9 trimethylation; OS, overall survival; PDAC, pancreatic ductal adenocarcinoma; RUVBL1, RuvB Like AAA ATPase 1; SETD1A, SET domain containing 1A, histone lysine methyltransferase.

1 | INTRODUCTION

The incidence and mortality of pancreatic ductal adenocarcinoma (PDAC) have been increasing worldwide every year.[1] While several chemotherapy protocols for PDAC have been developed, it is still one of the most aggressive malignancies. Patient prognosis is poor,[2] especially for patients diagnosed with unresectable PDAC, with a median survival of approximately 4 months and a 5-year survival rate of 3%.[3] To improve the prognosis of patients with PDAC, it is necessary to elucidate its biomolecular characteristics, especially the epigenomic abnormalities.[4]

Histone modification is an important epigenetic mechanism that plays an essential role in the regulation of gene expression, which is intimately connected to the development and progression of diseases, including cancer.[5,6] Histone methylation of the lysine (K) residue in the histone H3 tail has been widely investigated. H3K9 trimethylation (me3) and H3K27me3 at the gene promoter region are linked to gene inactivation,[7] which is catalyzed by EZH2 and SETDB1 /SUV39H1, respectively[8] High expression of EZH2 is associated with a worse prognosis in patients with PDAC.[9] SETDB1 knockout led to increased p53-mediated apoptosis, resulting in suppression of PDAC formation and a better prognosis in a mouse model.[10] In contrast, H3K4me3 is associated with transcriptional activation of genes and is catalyzed by various enzymes, such as MLL1/2/3, SETD1A, and SETD1B.[8] Somatic mutations of the MLL2/3 gene were found in PDAC tissues, but their mutation frequencies are relatively low (5–7%).[11] However, the effects of the enzymes that catalyze H3K4me3 on clinicopathological factors remain largely unknown.

SETD1A (SET domain containing 1A, histone lysine methyltransferase) and its paralog SETD1B are members of the SET1/Complex Proteins Associated with Set1 (COMPASS) complex family that is widely conserved from yeast to human.[12] SETD1A is localized in the nucleus, but SETD1B is mostly in the cytoplasm, suggesting that the two have distinct functions.[13] The SET1A/COMPASS complex regulates transcriptional gene activation through H3K4 methylation in embryonic stem cell renewal and differentiation.[14] SETD1A has also been shown to be essential for maintaining mitosis and cell proliferation.[15] According to previous studies, SETD1A expression is upregulated in various cancers, and its overexpression accelerates cell proliferation, invasiveness, and tumorigenicity.[16–18] Although SETD1A contributes to genome-wide H3K4me3 deposition and some target genes of SETD1A were recently found in gastric cancer cells,[19] the molecular mechanism underlying SETD1A overexpression as well as the target genes associated with H3K4me3 have not yet been elucidated in PDAC.

In this study, we demonstrated that SETD1A overexpression is frequently observed in PDAC tissues and is associated with a poor prognosis. Additionally, an oncogenic protein ATP-dependent DNA helicase, *RUVBL1* (*RuvB Like AAA ATPase 1*), was identified as a novel transcriptional target gene of SETD1A histone methyltransferase in PDAC cells. Mechanicolorectalstically, SETD1A overexpression enhanced cell growth and invasiveness via the SETD1A-H3K4me3-*RUVBL1* pathway. Clinical co-expression of SETD1A and *RUVBL1* is an independent prognostic factor, indicating the significance of this pathway in PDAC patients.

2 | MATERIALS AND METHODS

2.1 | Human tissue samples

A total of 105 patients who underwent radical pancreatectomy for PDAC at Tokyo Medical and Dental University Hospital between 2007 and 2018 were included in this study. Written informed consent was obtained from all patients with the approval of the Ethics Committee of Tokyo Medical and Dental University School of Medicine. The patients were coded anonymously in accordance with the ethical guidelines of the Declaration of Helsinki. The clinicopathological features of 105 PDAC patients are summarized in Tables S1–S3 and Appendix S1.

2.2 | Immunohistochemistry

Immunohistochemistry using formalin-fixed paraffin-embedded tissues was accomplished with a Histofine Simple Stain MAX PO system (Nichirei Biosciences, Tokyo, Japan) according to the manufacturer's protocol. The primary antibodies used were anti-SETD1A (1:200, NBP2-49281, Novus Biologicals) and anti-Pontin 52 (RUVBL1, 1:2000, sc-393,905, Santa Cruz Biotechnology). We utilized colorectal cancer tissues as positive controls for immunohistochemistry using anti-SETD1A and anti-RUVBL1 antibodies (Figure S1A). Rabbit IgG (Normal Rabbit IgG #2729, CST: Cell Signaling Technology) and mouse IgG (Normal Mouse IgG #5415, CST) were used as negative controls in place of anti-SETD1A rabbit polyclonal and anti-Pontin 52/RUVBL1 mouse monoclonal antibodies, respectively. According to previous studies on SETD1A,[20] immunohistochemical expression was evaluated with staining extent and intensity scores of 0–3 (Figure S1B), and samples were divided into high (scores 2–3) and low (scores 0–1) levels of SETD1A as well as RUVBL1.[21]

2.3 | Human cell lines

Seven PDAC cell lines (AsPC-1, PANC-1, BxPC-3, KLM-1, MIAPaCa-2, DAN-G, and PSN-1) were purchased from the American Type Culture Collection (ATCC), the European Collection of Authenticated Cell Cultures (ECACC), RIKEN BRC cell bank and the Human Science Research Resources Bank (HSRRB). A normal human pancreatic duct epithelial (HPDE) cell line was generously provided by Dr Ming-Sound Tsao (University of Toronto).[22] These cells were grown in an appropriate culture medium (Appendix S1).

2.4 | Knockdown experiments

Three small interfering RNAs (siRNAs) and negative control (Mission siRNA Universal Negative Control) were purchased from Merck KGaA. Each siRNA was transfected into PDAC cells to give a final concentration of 50 nM by using a Lipofectamine RNAiMAX Transfection Reagent (Invitrogen) according to the manufacturer's instructions. The sequences of *SETD1A* siRNA are follows: siSETD1A#1:5′-CAGCAGCUGUUUCCUGUGGAA -3′; siSETD1A#2: 5′- CUUUGCGGAGAAGAAGCUG- 3′; siSETD1A#3:5′ -GAACAGAU

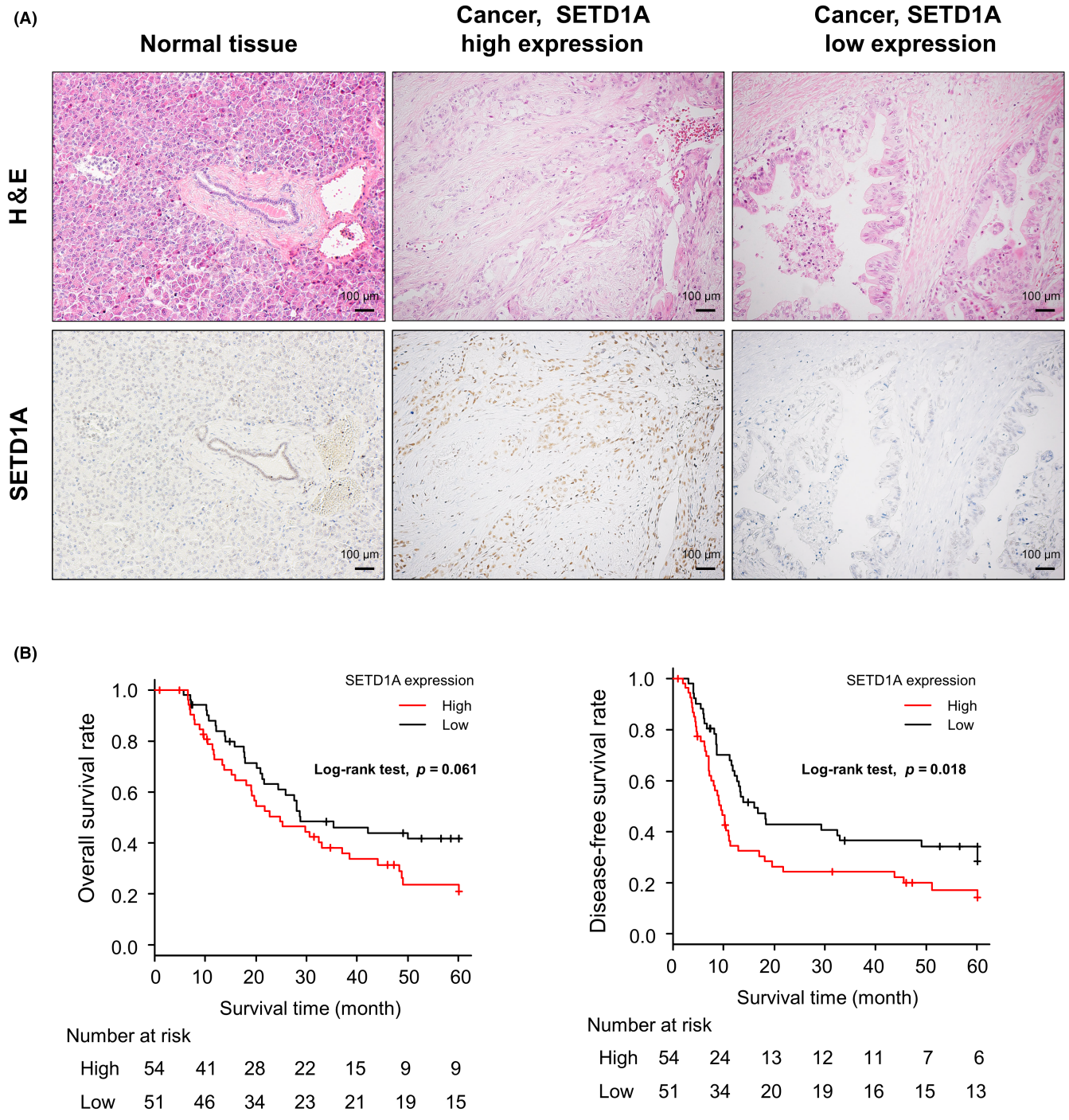

FIGURE 1 Evaluation of SETD1A expression in resected pancreatic cancer specimens. (A) Representative hematoxylin and eosin (HE) stain and immunohistochemistry images with anti-SETD1A antibody; from left to right, the normal tissue of pancreatic ducts in a pancreatic neuroendocrine tumor case, the pancreatic cancer tissue of SETD1A high expression case, and low expression case are shown. Original magnification ×100. (B) Kaplan–Meier curves of overall survival and disease-free survival of 105 clinical cases of pancreatic ductal adenocarcinoma (PDAC) grouped by SETD1A expression. *p*-value was calculated using the log-rank test

GACCAUCCUGU- 3′. *RUVBL1* siRNA (SASI_Hs01_00131544, Merck), which was validated by Assimon et al.,[23] was also transfected into PDAC cells. After 48–72 h culturing, transfected cells were harvested and used for gene expression and functional analyses.

2.5 | Establishment of SETD1A- and RUVBL1-overexpressed PDAC cell lines

The PCR product of the entire coding sequence of *SETD1A* and *RUVBL1* were cloned into the CSII-EF-MCS-IRES-Puro plasmid,[24,25] and established the PDAC cell lines with their overexpression, as shown in Appendix S1.

2.6 | Cell proliferation, cell migration, and invasion assays

To assess the cell proliferation, WST-8 assay, a water-soluble tetrazolium salt used for assessing cell metabolic activity, was conducted using Cell Counting Kit-8 (CCK-8) (CK04, Dojindo Kumamoto). Migration and invasion assays were performed using cell culture insert chambers (without Matrigel) and BioCoat Matrigel invasion chambers (with Matrigel), respectively (8.0 μm PET membrane, Corning). Detailed methods are shown in Appendix S1.

2.7 | RNA-seq, RT-PCR, chromatin immunoprecipitation (ChIP) and western blot

The detailed methods are shown in Appendix S1. The primer sets for RT-PCR and qChIP-PCR are listed in Table S4.

2.8 | Animal experiments

Tumorigenicity was assessed by using DAN-G cells, which had high tumorigenic activity (Wagner et al. Clin Cancer Res 2008),[26] as shown in Appendix S1. Immunodeficient nude mice (KSN/Slc, male, 4 weeks old) were purchased from Japan SLC. All mouse procedures were approved by the Institutional Animal Care and Use Committee of the Tokyo Medical and Dental University and conducted according to its guidelines.

2.9 | Statistical analysis

Statistical analyses were performed using EZR (version 3.1.1; Saitama Medical Center, Jichi Medical University), a graphical user interface for R (R Foundation for Statistical Computing). A two-sided Student's *t*-test was used to analyze the differences between the continuous values of the two independent groups. The χ^2 test or Fisher's exact test was used for the analysis of categorical variables. Survival curves were calculated using the Kaplan–Meier method and compared using the log-rank test or the generalized Wilcoxon test. $p < 0.05$ was considered statistically significant.

3 | RESULTS

3.1 | Evaluation of SETD1A expression in pancreatic cancer cell lines and SETD1A immunohistostaining of PDAC tissues

Immunohistochemical staining was performed to detect SETD1A protein expression in 105 resected PDAC specimens. Basal expression of SETD1A in normal pancreas was low, and PDAC cells showed relatively higher expression of SETD1A than normal pancreas. High expression of SETD1A was detected in 54 PDAC tissues (51.4%) (Figure 1A). There were no statistically significant differences between SETD1A and the clinicopathological characteristics of PDAC, except for venous invasion ($p = 0.002$, Table S1). The high SETD1A expression group tended to have a poor overall survival (OS) ($p = 0.061$) and significantly shorter DFS than the low SETD1A expression group ($p = 0.018$) (Figure 1B). In the univariate analysis, several factors, such as lymph node metastasis, tumor size, and tumor markers, contributed to DFS. Moreover, in the multivariate analysis, increased expression of SETD1A was a significant independent prognostic factor following lymph node metastasis (Tables S2 and S3). The presence of adjuvant and neoadjuvant chemotherapy was not associated with SETD1A expression in PDAC.

3.2 | Evaluation of biological effect by SETD1A knockdown on PDAC cells

Next, we examined SETD1A expression levels in seven PDAC cell lines and an HPDE cell line derived from normal pancreatic duct

FIGURE 2 Evaluation of the biological effect of SETD1A knockdown on pancreatic cancer cells. (A, B) qRT-PCR (A) and Western blot (B) analyses of SETD1A expression in seven pancreatic cancer cell lines and a normal human pancreatic duct epithelial (HPDE) cell line. Relative *SETD1A* mRNA expression levels were normalized to *GAPDH* (A). Error bars indicate the mean ± SE. The expression ratio of SETD1A quantified by ImageJ 1.53e software using GAPDH expression of each cell as an internal control is also shown (B). (C) Cell proliferation assays for the pancreatic ductal adenocarcinoma (PDAC) cells (AsPC-1 and PANC-1) with *SETD1A* knockdown (KD) ($n = 8$). Error bars indicate the mean ± SE. (D) Colony formation assay for the *SETD1A*-KD PDAC cells ($n = 3$). The left panels show the images of the colonies, and the right panels show the bar graphs of the mean number of counted colonies. Error bars indicate the mean ± SE. (E, F) Migration assay (E) and invasion assay (F) in *SETD1A*-KD PDAC cells. The left panels show the representative images. The number of migrating and invading cells was counted on the membrane ($n = 3$), and then the average number of cells was calculated. Error bars indicate the mean ± SE. Student's *t* test, $^{*}p < 0.05$; $^{**}p < 0.01$; $^{***}p < 0.001$

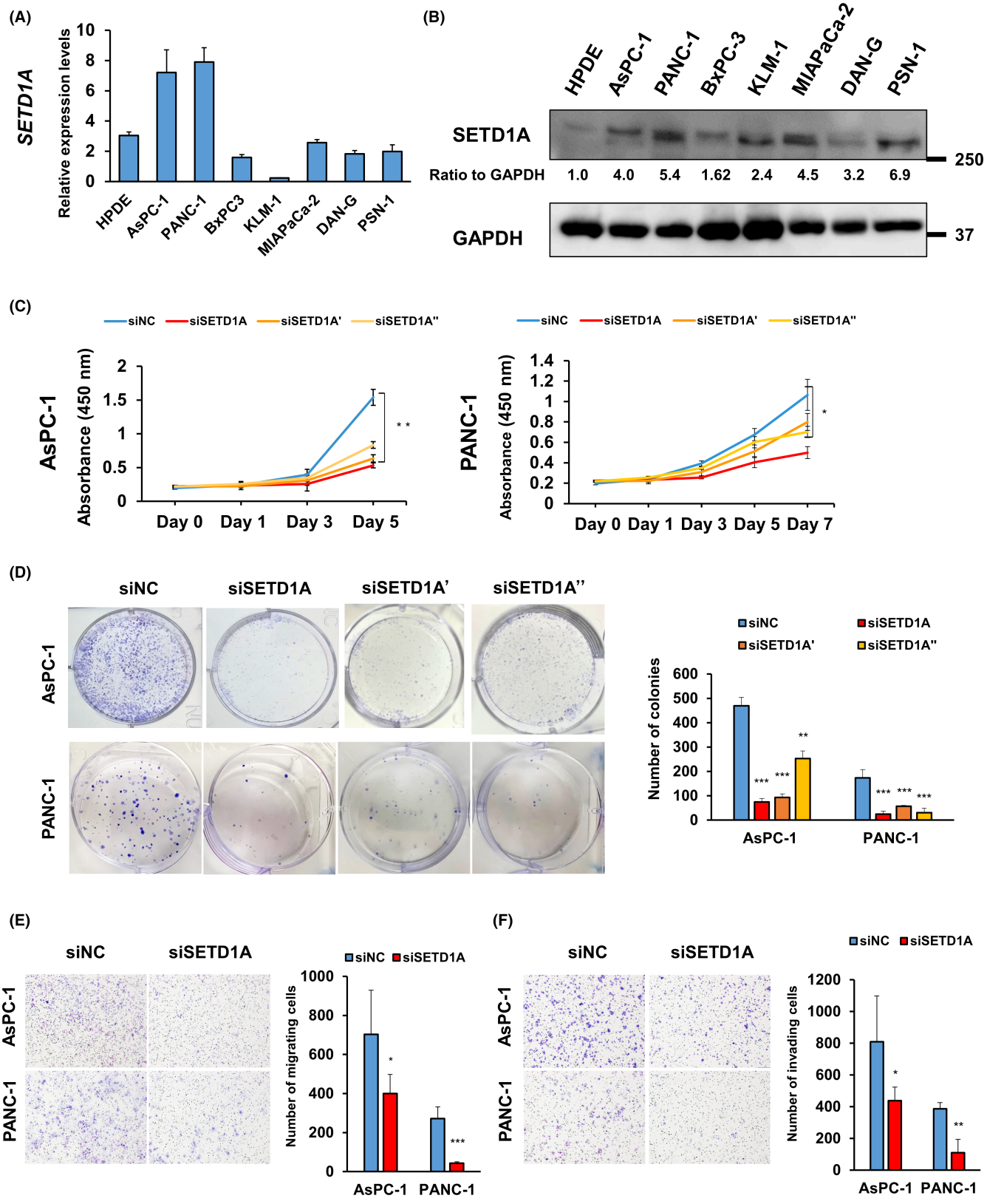

cells using RT-PCR and western blotting. Although several PDAC cells showed distinct expression between mRNA and protein levels, AsPC-1 and PANC-1 cells showed higher SETD1A among the PDAC cells (Figure 2A,B).

To analyze the functional role of SETD1A, we performed siRNA-based knockdown in AsPC-1 and PANC-1 cells using three siRNAs, named siSETD1A, siSETD1A′ and siSETD1As″, and evaluated their effects on cell proliferation and invasion ability. Transfection with

all three siRNAs of SETD1A inhibited both mRNA and protein expression (Figure S2A,B). Our results were consistent with those of previous studies reporting that CDH1 (E-cadherin) expression was upregulated after the knockdown of *SETD1A* (Figure S2B).[16,19] In addition, knockdown of *SETD1A* significantly inhibited the proliferation of each cell line according to the WST-8 and colony formation assays (Figure 2C,D). Migration and invasion were also inhibited in both AsPC-1 and PANC-1 cells following *SETD1A* knockdown (Figure 2E,F, Figure S2C,D). These results indicate that the inhibition of SETD1A leads to a decrease in cell proliferation, migration, and invasion.

3.3 | Identification and ChIP analysis of genes that are upregulated or downregulated upon SETD1A-knockdown

To investigate the epigenetic function of SETD1A, we searched for SETD1A downstream target genes in two pancreatic cancer cell lines, AsPC-1 and PANC-1, using RNA-seq analysis after siSETD1A-based knockdown, which was most effective for cell proliferation (Figure 2). As a result, we identified 10 commonly downregulated genes (*TMEM164*, *TRMT2B*, *TRAPPC6A*, *L3MBTL2*, *RUVBL1*, *ZNF146*, *NID1*, *TMEM250*, *ELOA*, and *UROS*) and four upregulated genes (*CDH1*, *CDH3*, *B3GNT5*, and *PLAU*) in these two cell lines, when the fold changes of gene expression levels were logFC ≤ −1.2 and logFC ≥ 1.2 compared to the control (Figure 3A,B and Table S5). We then confirmed the changes in expression of these common genes in AsPC-1 and PANC-1 with three SETD1A siRNAs using qRT-PCR analysis (Figure 3C,D, Figure S2E).

SETD1A is an H3K4 methyltransferase associated with the transcriptional activation of genes.[8] Among the 10 commonly downregulated genes detected in our study, four genes (*L3MBTL2*, *RUVBL1*, *ZNF146*, and *NID1*) were reported to be associated with cell proliferation, but there are no reports about function and expression changes of the remaining six genes in cancer. To evaluate whether these genes are directly regulated by SETD1A, we performed quantitative ChIP-PCR (qChIP-PCR) analysis of SETD1A occupancy and H3K4me3 levels at the promoter regions of the four target genes. The SETD1A binding and H3K4me3 levels at the *RUVBL1* promoter region were significantly decreased in the two cell lines with *SETD1A* knockdown using each of the three types of siRNA (Figure 3E). Among the remaining three genes, *SETD1A* knockdown exhibited an obvious reduction of the SETD1A binding and H3K4me3 levels at the *L3MBLT2* promoter in AsPC-1 cells and tended to show in PANC1 cells (Figure 3E).

3.4 | Evaluation of the biological effects of SETD1A overexpression on PDAC cells

We established DAN-G and KLM-1 cells that stably overexpressed *SETD1A*. RT-PCR, and western blotting showed marked upregulation of SETD1A and significant upregulation of *RUVBL1* in *SETD1A*-overexpressing cells (Figure 4A,B). In addition, both *SETD1A*-overexpressing DAN-G and KLM-1 cells had significantly increased cell proliferation compared to GFP-expressing control cells (Figure 4C,D). Moreover, xenograft tumors from *SETD1A*-overexpressing DAN-G cells grew faster than those from control cells ($p < 0.001$, Figure 4E). Higher SETD1A and RUVBL1 expression was observed in *SETD1A*-overexpression-derived xenograft tumors (Figure 4E), indicating a positive correlation between SETD1A and RUVBL1 in an in vivo model. Upregulation of *RUVBL1* was observed in HEK293T cells transiently overexpressing SETD1A (Figure 4F,G), and the SETD1A binding and H3K4me3 levels were significantly increased at the *RUVBL1* promoter region in the cells (Figure 4H). These results suggested that *RUVBL1* is a direct target of SETD1A.

3.5 | Evaluation of the biological effect of RUVBL1 expression on PDAC cells

SETD1A knockdown attenuated *RUVBL1* mRNA and protein expression in AsPC-1 and PANC-1 cells (Figure 3C,D and 5A). To assess whether RUVBL1 is involved in the decreased cell proliferation and invasiveness of pancreatic cancer cells with *SETD1A* knockdown, we evaluated the effects of *RUVBL1* knockdown in these two cell lines by using the validated siRNA,[23] as shown in Figure 5B,C. *RUVBL1* knockdown suppressed the proliferation, migration, and invasion of PDAC cells (Figure 5D–F). The proliferative capacity was significantly reduced in SETD1A-overexpressing DAN-G and KLM-1 cells when *RUVBL1* expression was inhibited by its siRNA transfection (Figure 5G and Figure S3). In contrast, overexpression of *RUVBL1*

FIGURE 3 Identification and analysis of genes that are upregulated or downregulated upon SETD1A-knockdown. (A, B) Venn diagrams show genes whose expression was downregulated (A) and upregulated (B) by knockdown (KD) using si*SETD1A* in AsPC-1 and PANC-1 cells. (C, D) qRT-PCR of downregulated and upregulated genes by *SETD1A*-KD in PDAC cells. The expression levels of downregulated (C) and upregulated (D) genes were confirmed in PDAC cells after siSETD1A transfection. Relative expression levels of each gene were normalized to *GAPDH*. (E) Quantitative ChIP analysis of the SETD1A binding and H3K4me3 levels at the promoter regions of four genes commonly downregulated by *SETD1A*-KD in AsPC-1 and PANC-1 cells. The upper panels show a schematic representation of the 5′-regions of *L3MBTL2*, *RUVBL1*, *ZNF146*, and *NID1*. Open and closed boxes demonstrate the untranslated and translated regions, respectively. Curved arrow indicates transcription start site (TSS), and the double arrows are the ChIP sites in this study. After transfection of three siRNAs into AsPC-1 and PANC1 cells, ChIP was performed using anti-SETD1A, anti-Histone H3 antibody, and anti-H3K4me3 antibody. The relative levels of SETD1A binding to the promoter were normalized to Input DNA (% of Input), and enrichments of H3K4me3 were normalized to pan H3. qChIP- and qRT-PCR was performed in triplicate ($n = 3$). Boxes are the mean ± SE. Student's *t* test, $^{*}p < 0.05$; $^{**}p < 0.01$; $^{***}p < 0.001$

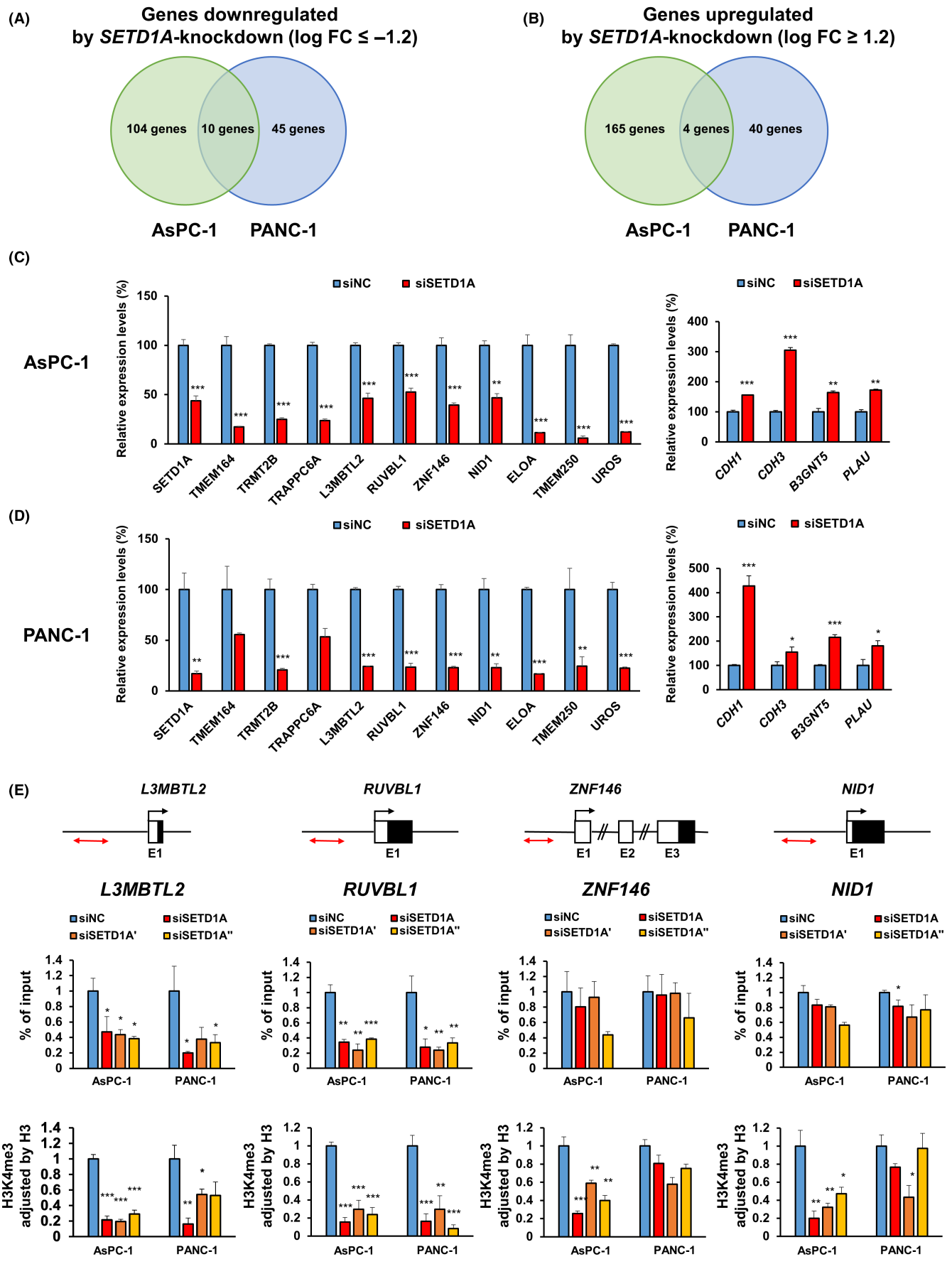
(A)
Genes downregulated by SETD1A-knockdown (log FC ≤ –1.2)
104 genes
10 genes
45 genes
AsPC-1
PANC-1
(B)
Genes upregulated by SETD1A-knockdown (log FC ≥ 1.2)
165 genes
4 genes
40 genes
AsPC-1
PANC-1
(C)
AsPC-1
siNC
siSETD1A
Relative expression levels (%)
SETD1A
TMEM164
TRMT2B
TRAPPC6A
L3MBTL2
RUVBL1
ZNF146
NID1
ELOA
TMEM250
UROS
CDH1
CDH3
B3GNT5
PLAU
(D)
PANC-1
(E)
L3MBTL2
RUVBL1
ZNF146
NID1
E1
E2
E3
siSETD1A'
siSETD1A''
% of input
H3K4me3 adjusted by H3

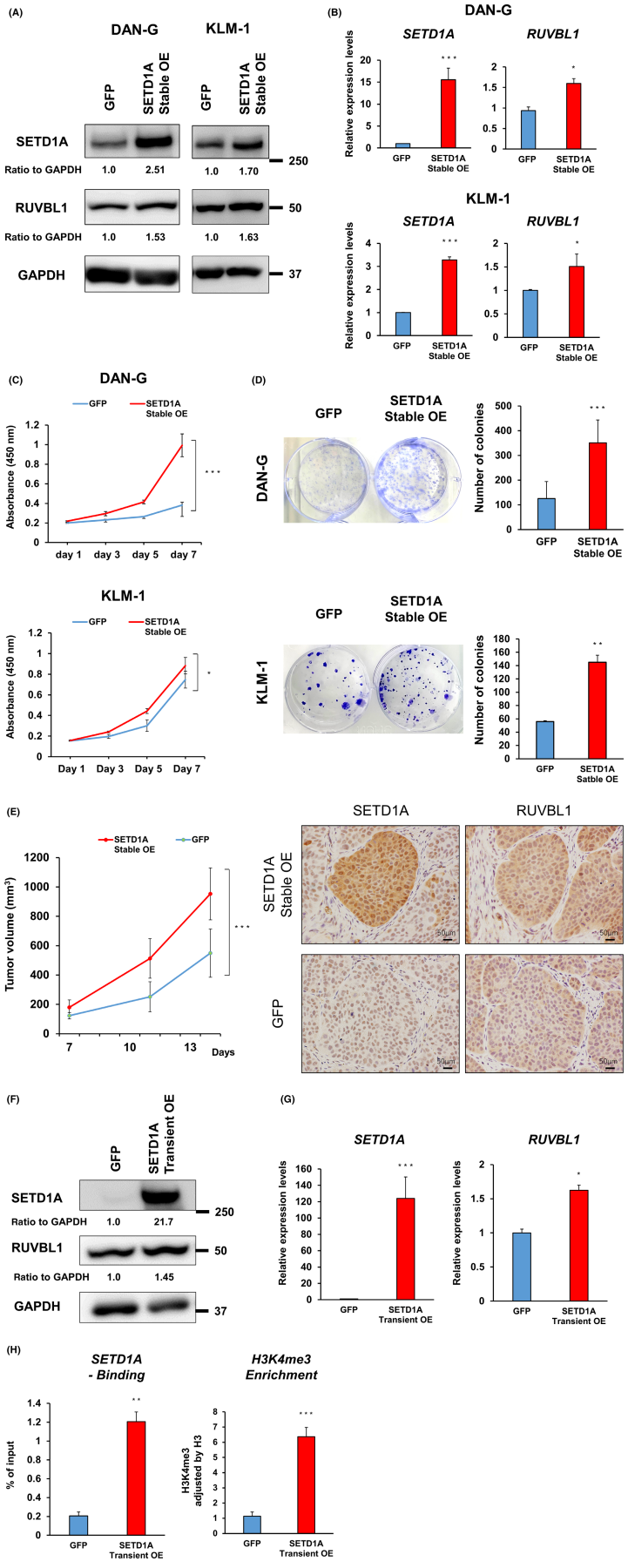

FIGURE 4 Evaluation of biological effects of SETD1A overexpression on pancreatic cancer cells. (A) Western blot analysis of SETD1A and RUVBL1 in DAN-G and KLM-1 cells stably overexpressed (OE) *SETD1A* or *GFP* with HA tag by a lentivirus expression vector system. GAPDH was used as loading control. The relative levels were analyzed using the ImageJ 1.53e software. (B) RT-PCR of *SETD1A* and *RUVBL1* in *SETD1A*-OE DAN-G and KLM-1 cells. qRT-PCR was performed in triplicate. Relative expression levels were normalized to *GAPDH*. (C) Cell proliferation assays for the *SETD1A*-OE PDAC cells ($n = 6$). Error bars indicate the mean ± SE. (D) Colony formation assay for the *SETD1A*-OE PDAC cells ($n = 3$). The left panels show the images of the colonies, and the right panels show the bar graphs of the mean number of counted colonies (D). Error bars indicate the mean ± SE. (E) The xenograft mouse models of *SETD1A*-OE DAN-G cells. Subcutaneous tumors were measured for 14 days from after injection (left), and then mice were killed. Immunohistochemistry images of their tumor with SETD1A and RUVBL1(right). Original magnification ×200. (F, G) Western blot (F) and qRT-PCR (G) analyses of SETD1A and RUVBL1 in HEK293T cells with transiently expressed *GFP* or *SETD1A* with HA tag. (H) Quantitative ChIP analysis of the SETD1A binding and H3K4me3 levels at the *RUVBL1* promoter region in HEK293T cells with transiently expressed HA-SETD1A. The *RUVBL1* promoter region was amplified (Figure 3E), and their relative levels of SETD1A binding and H3K4me3 were normalized to Input DNA and pan H3, respectively. qChIP- and qRT-PCR was performed in triplicate ($n = 3$). Error bars are mean ± SE. Student's *t* test, $^{*}p < 0.05$; $^{**}p < 0.01$; $^{***}p < 0.001$

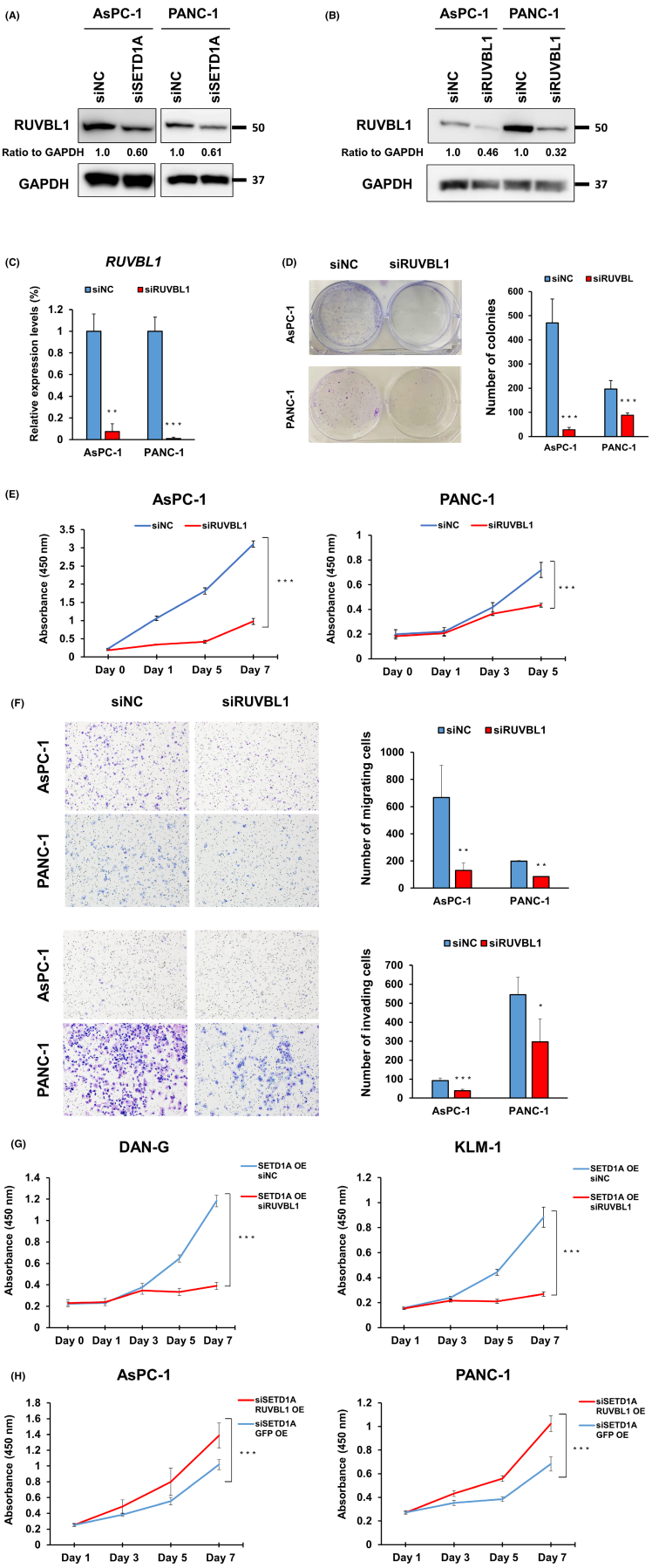

FIGURE 5 Evaluation of biological effect by RUVBL1 knockdown on pancreatic cancer cells. (A, B) Western blot analysis of RUVBL1 in AsPC-1 and PANC-1 cells after *SETD1A* (A) or *RUVBL1* (B) knockdown (KD). GAPDH was used as loading control. The relative levels were analyzed using the ImageJ 1.53e software. (C) qRT-PCR of *RUVBL1* expression. *GAPDH* was used as an internal control. Error bars indicate the mean ± SE. (D) Colony formation for the *RUVBL1*-KD cells ($n = 3$). The left panels show the images of colonies, and the right panels show the bar graphs of the mean number of counted colonies. Error bars indicate the mean ± SE. (E) Cell proliferation assays for the *RUVBL1*-KD cells ($n = 6$). Error bars indicate the mean ± SE. (F) Migration assay and invasion assay in *RUVBL1*-KD PDAC cells. The left panels show the representative images of migrating (upper) and invading cells (lower). The number of migrating and invading cells was counted on the membrane ($n = 3$), and then the average number of cells was calculated (right). Error bars indicate the mean ± SE. (G) Cell proliferation assays for the SETD1A-OE PDAC cells after knockdown of *RUVBL1* ($n = 6$). Error bars indicate the mean ± SE. Student's *t* test, $^{*}p < 0.05$; $^{**}p < 0.01$; $^{***}p < 0.001$. (H) Effects on cell proliferation by RUVBL1 overexpression in PDAC cells with *SETD1A* knockdown ($n = 6$). Knockdown of SETD1A was performed using siSETD1A in AsPC1-1 and PANC-1 cells. The next day, RUVBL1 and GFP were transiently overexpressed in these cells. Error bars indicate the mean ± SE

rescued cell proliferation of PANC-1 and AsPC-1 cells reduced by *SETD1A* knockdown (Figure 5H and Figure S4). These data strongly suggest that *RUVBL1* upregulation by *SETD1A* overexpression promotes cell growth. In addition, we suppressed *L3MBTL2* expression by siRNA transfection in AsPC-1 cells; however, *L3MBTL2* knockdown did not inhibit cell growth (Figure S5).

3.6 | Association between SETD1A and RUVBL1 in clinical cases

Immunohistochemical staining of RUVBL1 in 105 resected PDAC cases showed that RUVBL1 expression was upregulated in 52 cases (49.5%; Figure 6A). We observed that RUVBL1 expression

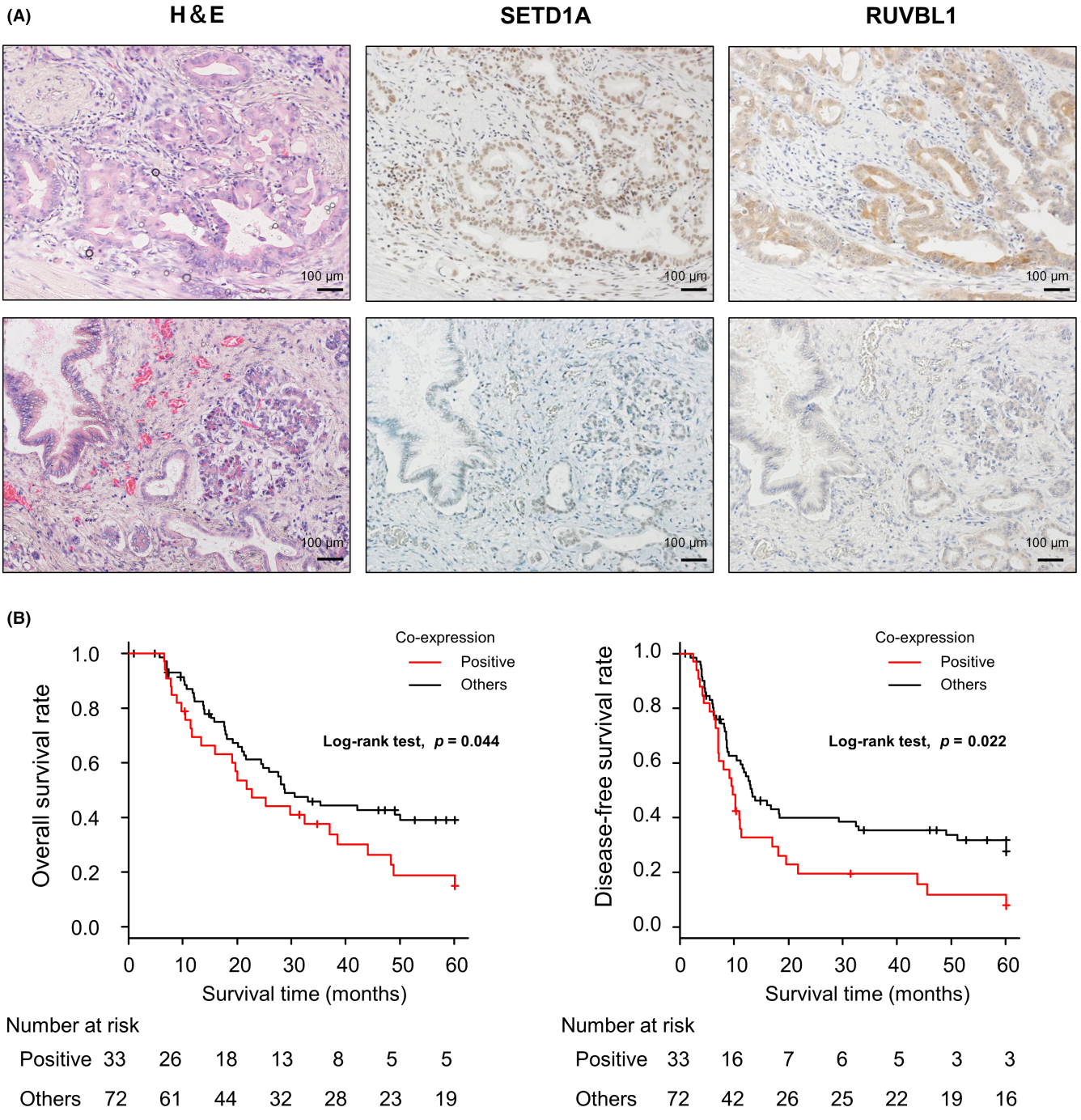

FIGURE 6 Correlation between SETD1A and RUVBL1 expression in primary pancreatic cancer. (A) Representative HE staining and immunohistochemical images of SETD1A and RUVBL1 staining in serial sections of the pancreatic cancer samples. The upper panels show images of a case with both high SETD1A and RUVBL1 expression, and the lower panels show images of a case with low expression. Original magnification ×100. (B) Kaplan–Meier curves for overall survival (left) and disease-free (right) survival of 105 clinical cases of pancreatic cancer. Positive co-expression means the high expression cases who had high expression of both SETD1A and RUBVL1. *p*-values were calculated using the log-rank test

was significantly correlated with SETD1A expression in PDAC tissues ($p = 0.032$; Table S6); however, RUVBL1 expression was not associated with DFS ($p = 0.15$) and OS ($p = 0.075$) (Tables S7 and S8). There was no statistically significant difference between the co-expression of these proteins and clinicopathological features (Table S9). However, PDAC patients with increased expression of both SETD1A and RUVBL1 had significantly shorter OS ($p = 0.044$) and DFS ($p = 0.022$) (Figure 6B). Multivariate analysis confirmed that the co-expression of SETD1A and RUVBL1 was a significant independent prognostic factor for DFS ($p = 0.046$) and OS ($p = 0.049$) (Tables 1 and 2). Our study revealed the clinical significance of the SETD1A/RUVBL1 pathway in patients with PDAC.

4 | DISCUSSION

Here we revealed that SETD1A was detected highly expressed in more than half (51.4%) of PDAC cases by immunohistochemistry, with the positive ratio of SETD1A similar to that in colorectal (67.8%), lung (48.9%) and breast (50.9%) cancer in the previous reports using immunohistochemistry.[20,27] As shown in Figure 1 and Table S1, SETD1A overexpression was correlated with venous invasion and worse prognosis with PDAC. A clinical association between SETD1A overexpression and poor survival has also been reported in cancers,[17,18,20] and higher SETD1A levels are associated with a more advanced clinical stage, vascular invasion, and metastasis in triple-negative breast cancer.[27] Therefore, SETD1A plays a pivotal role in the malignant progression of diverse cancer types, including PDAC.

SETDA1 overexpression was associated with DFS ($p = 0.018$) and tended to be correlated with OS ($p = 0.061$) of the patients with PDAC based on immunohistochemistry. We evaluated the relationship between *SETD1A* mRNA expression and the prognosis of PDAC patients using four public databases, The Cancer Genome Atlas (TCGA), GSE17891, GSE28735, and GSE62452, but Kaplan–Meier analysis on the expression level of SETD1A and DFS as well as OS did not show statistically significant difference by log-rank test ($p > 0.1$, Figure S6), indicating that SETD1A protein overexpression, not transcriptional overexpression, may be useful as a predictor of poor prognosis of PDAC patients. SETD1A is reported to be overexpressed at the mRNA and protein levels through multiple pathways. *SETD1A* is a downstream transcriptional target gene of the Wnt-β-catenin pathway in lung cancer,[28] and miR-324-3p downregulates *SETD1A* mRNA by binding to the *SETD1A* 3′-untranslated region in breast cancer.[29] Growing evidence shows the translational regulatory mechanism and protein stability of SETD1A. N^6-methyladenosine (m^6A) mRNA regulation via METTL14-METTL3-WTAP complex is reported to enhance the translation of genes, including SETD1A in erythroleukemia cells.[30] ES cells lacking CXXC finger protein 1 (Cfp1) decrease SETD1A expression at the protein level; the expression is recovered by treatment with the proteasome inhibitor MG132.[31] Further investigation is needed to uncover the regulatory mechanism of SETD1A expression in PDAC.

In our study on PDAC cells, inhibition of *SETD1A* reduced the proliferation and invasiveness of PDAC cells, whereas overexpression of *SETD1A* promoted cell proliferation as well as tumorigenicity and conferred an aggressive PDAC phenotype. These biological properties of *SETD1A* overexpression in PDAC cells may be caused by alterations of *SETD1A* downstream pathway because the *SETD1A*

TABLE 1 Univariate and multivariate analysis of clinicopathological factors contributing to disease-free survival

	Univariate analysis			Multivariate analysis		
Clinicopathological factors	**HR**	**95% CI**	***p***	**HR**	**95% CI**	***p***
Age, >70 years	0.98	0.62–1.56	0.95			
Gender, male	0.92	0.5805–1.45	0.72			
CEA, >5 ng/mL	1.63	1.64–1.02	0.039*	1.10	0.66–1.84	0.71
CA19-9, >37 U/mL	1.85	1.09–3.16	0.024*	1.36	0.77–2.42	0.29
Operative procedure, PD	1.17	0.75–1.83	0.50			
Differentiation, poorly differentiated	1.15	0.73–1.80	0.56			
Venous invasion, present	2.38	0.75–7.57	0.14			
Lymphatic vessel invasion, present	2.20	1.38–3.50	0.0010*	1.25	0.72–2.18	0.43
UICC T status, ≥T3	1.62	0.99–2.62	0.052			
UICC N status, ≥N1	3.44	2.00–5.91	<0.001*	3.00	1.58–5.74	<0.001*
UICC M status, M1	2.02	0.87–4.70	0.10			
Adjuvant chemotherapy, present	1.99	0.99–3.99	0.052			
Neoadjuvant chemotherapy, present	1.23	0.39–3.92	0.72			
Co-expression of SETD1A and RUVBL1, present	1.71	1.08–2.73	0.023*	1.65	1.01–2.71	0.046*

Abbreviations: CI, confidence interval; DP, pancreaticoduodenectomy; HR, hazard ratio; PD, pancreaticoduodenectomy; TP, total pancreatectomy; UICC, Union for International Cancer Control.

*Indicates statistical significance ($p < 0.05$).

TABLE 2 Univariate and multivariate analysis of clinicopathological factors contributing to overall survival

	Univariate analysis			Multivariate analysis		
Clinicopathological factors	HR	95% CI	*p*	HR	95% CI	*p*
Age, >70 years	1.05	0.64–1.73	0.84			
Gender, male	1.01	0.61–1.66	0.97			
CEA, >5 ng/mL	1.91	1.16–3.14	0.011*	1.49	0.89–2.52	0.13
CA19-9, >37 U/mL	1.41	0.81–2.46	0.23			
Operative procedure, PD	1.10	0.68–1.78	0.70			
Differentiation, poorly differentiated	1.456	0.89–2.37	0.13			
Venous invasion, present	2.98	0.73–12.1	0.13			
Lymphatic vessel invasion, present	2.07	1.24–3.44	0.0052*	1.09	0.61–1.98	0.77
UICC T status, ≥T3	1.81	1.08–3.02	0.024*	1.38	0.81–2.35	0.23
UICC N status, ≥N1	3.86	2.09–7.14	<0.001*	3.32	1.61–6.89	0.0011*
UICC M status, M1	3.86	2.09–7.14	0.15			
Adjuvant chemotherapy, present	0.61	0.34–1.11	0.11			
Neoadjuvant chemotherapy, present	2.00	0.63–6.44	0.24			
Co-expression of SETD1A and RUVBL1, present	1.66	1.01–2.72	0.046*	1.68	1.00–2.83	0.049*

Abbreviations: CI, confidence interval; DP, pancreaticoduodenectomy; HR, hazard ratio; PD, pancreaticoduodenectomy; TP, total pancreatectomy; UICC, Union for International Cancer Control.

*Indicates statistical significance ($p < 0.05$).

target genes detected in our RNA-seq analysis, such as *RUVBL1*, *L3MBLT2*, *ZNF146*, and *NID1*, are known to increase cancer growth, invasion, and metastasis.[32–35]

Compelling evidence indicates that SETD1A participates in the transcriptional activation of genes through the elevated occupation of H3K4me3 at the gene promoter.[36] *Estrogen* receptor α and *FOXM1* are also known as the direct targets of *SETD1A* through H3K4me3 in breast and prostate cancer.[37,38] We found that the levels of *SETD1A* occupancy and H3K4me3 enrichment were decreased at the *RUVBL1* promoter region in PDAC cells with *SETD1A* knockdown and vice versa in HEK293T cells with *SETD1A* overexpression, indicating that *RUVBL1* is a direct downstream target gene of *SETD1A* by increasing H3K4me3. While Baron et al. revealed that *RUVBL1* was upregulated by *BCL6* knockdown in lymphoma,[39] Chen et al. reported that the *circMYO10/miR-370-3p* axis promoted *RUVBL1* expression in osteosarcoma.[40] Our findings provide new insights into the transcriptional regulatory mechanism of *RUVBL1* via the epigenetic pathway of SETD1A.

RUVBL1 physiologically interacts with numerous factors, such *ß-catenin* and *c-Myc/Miz-1*, and thereby plays roles in both transcriptional activation and repression, chromatin remodeling, DNA damage response, telomerase activity, and cell deformation.[32,41–43] RUVBL1 is overexpressed in many cancer types, which is involved in the oncogenic process.[23,44,45] As demonstrated in Figures 2 and 5, inhibition of cell proliferation and invasiveness were observed after knockdown of RUVBL1 in PDAC cells, which was similar to that of SETD1A. Moreover, *SETD1A*-overexpressing DAN-G cells accelerated tumor growth with increased *RUVBL1* expression in mouse xenograft model, supporting the biological importance of SETD1A-RUVBL1 pathway in PDAC cells.

Since there is a significant positive correlation between SETD1A and RUVBL1 expression in clinical samples, RUVBL1 might be a potential target of SETD1A in PDAC. It is worth noting that PDAC patients with both SETD1A and RUVBL1 expression had a significant difference in DFS and OS (Figure 6, Tables 1 and 2). Therefore, co-overexpression of SETD1A and RUVBL1 may be a useful biomarker for predicting survival of PDAC patients. Indeed, small-molecule inhibitors targeting the SET1 family as well as RUBVL1 have been developed as anti-cancer drugs for several cancers.[23,46,47] Combination treatment with SETD1A and RUVBL1 inhibitors may serve as a novel therapeutic approach for patients with PDAC.

In conclusion, we discovered that SETD1A expression is upregulated in more than half of PDAC patients and shows significantly positive correlation to RUVBL1 overexpression in PDAC tissues. SETD1A overexpression is an independent prognostic factor in conditions where it is also upregulated by RUVBL1. Our data suggest that RUVBL1 is a novel downstream target of SETD1A-dependent H3K4me3, whose pathway plays an essential role in controlling cell proliferation of PDAC cells. Knockdown of SETD1A in PDAC cells attenuates cell proliferation and invasion through RUVBL1 downregulation, suggesting that inhibition of the SETD1A-H3K4me3-RUVBL1 pathway may be a promising therapeutic strategy for the treatment of PDAC.

AUTHOR CONTRIBUTIONS

T.I, Y.A: Acquisition of the data, statistical analysis, drafting of the paper. Y.A: Construction of vectors, conceptualized the study. S.S: Bioinformatics, advice for experiments. A.K, H.O: Advice for experiments. D.A, S.W, Y.I, H.U, K.A, K.O, H.O, A.K, M.T: Provision of clinical samples, elaboration of the manuscript. S.T: Conceptualized, designed and supervised the study.

ACKNOWLEDGMENTS

We gratefully thank Ms Hiromi Nagasaki and Ms Michiko Mizuno for technical and clerical assistance.

FUNDING INFORMATION

This work was supported by Grants-in-Aid for Scientific Research (A; 19H01055, B; 20H03526) and Challenging Research (Exploratory; 20K21627) from the Ministry of Education, Culture, Sports, Science and Technology of Japan; Research Grant from the Princess Takamatsu Cancer Research Fund; and P-CREATE (JP19cm0106540) from AMED (Japan Agency for Medical Research and Development).

DISCLOSURE

The authors have no conflict of interest. Shinji Tanaka is an editorial board member of *Cancer Science*.

ETHICAL APPROVAL

- Approval of the research protocol by an Institutional Reviewer Board: This study was approval by the Ethics Committee of Tokyo Medical and Dental University School of Medicine (permission number G2017-018) and was conducted in accordance with the Declaration of Helsinki.
- Informed Consent: Written informed consent was obtained from all patients.
- Registry and the Registration No. of the study/trial: N/A.
- Animal Studies: All mouse procedures were approved by the Institutional Animal Care and Use Committee of the Tokyo Medical and Dental University (permission number: A2017-269C).

ORCID

Shu Shimada https://orcid.org/0000-0002-4962-0636
Hiroaki Ono https://orcid.org/0000-0001-9230-5714
Shinji Tanaka https://orcid.org/0000-0002-7718-3453

REFERENCES

1. Collaborators GBDPC. The global, regional, and national burden of pancreatic cancer and its attributable risk factors in 195 countries and territories, 1990-2017: a systematic analysis for the global burden of disease study 2017. Lancet. *Gastroenterol Hepatol*. 2019;4:934-947.
2. Neoptolemos JP, Kleeff J, Michl P, Costello E, Greenhalf W, Palmer DH. Therapeutic developments in pancreatic cancer: current and future perspectives. *Nat Rev Gastroenterol Hepatol*. 2018;15:333-348.
3. Siegel RL, Miller KD, Jemal A. Cancer statistics, 2018. *CA Cancer J Clin*. 2018;68:7-30.
4. Lomberk G, Dusetti N, Iovanna J, Urrutia R. Emerging epigenomic landscapes of pancreatic cancer in the era of precision medicine. *Nat Commun*. 2019;10:3875.
5. Dawson MA, Kouzarides T. Cancer epigenetics: from mechanism to therapy. *Cell*. 2012;150:12-27.
6. Suvà ML, Riggi N, Bernstein BE. Epigenetic reprogramming in cancer. *Science*. 2013;339:1567-1570.
7. Zhao Z, Shilatifard A. Epigenetic modifications of histones in cancer. *Genome Biol*. 2019;20:245.
8. Fritsch L, Robin P, Mathieu JR, et al. A subset of the histone H3 lysine 9 methyltransferases Suv39h1, G9a, GLP, and SETDB1 participate in a multimeric complex. *Mol Cell*. 2010;37:46-56.
9. Hasegawa S, Nagano H, Konno M, et al. A crucial epithelial to mesenchymal transition regulator, Sox4/Ezh2 axis is closely related to the clinical outcome in pancreatic cancer patients. *Int J Oncol*. 2016;48:145-152.
10. Ogawa S, Fukuda A, Matsumoto Y, et al. SETDB1 inhibits p53-mediated apoptosis and is required for formation of pancreatic ductal adenocarcinomas in mice. *Gastroenterology*. 2020;159:682-696.e613.
11. Sausen M, Phallen J, Adleff V, et al. Clinical implications of genomic alterations in the tumour and circulation of pancreatic cancer patients. *Nat Commun*. 2015;6:7686.
12. Cenik BK, Shilatifard A. COMPASS and SWI/SNF complexes in development and disease. *Nat Rev Genet*. 2021;22:38-58.
13. Sugeedha J, Gautam J, Tyagi S. SET1/MLL family of proteins: functions beyond histone methylation. *Epigenetics*. 2021;16:469-487.
14. Meeks JJ, Shilatifard A. Multiple roles for the MLL/COMPASS family in the epigenetic regulation of gene expression and in cancer. *Annu Rev Cancer Biol*. 2017;1:425-446.
15. Tajima K, Matsuda S, Yae T, et al. SETD1A protects from senescence through regulation of the mitotic gene expression program. *Nat Commun*. 2019;10:2854.
16. Salz T, Li G, Kaye F, Zhou L, Qiu Y, Huang S. hSETD1A regulates Wnt target genes and controls tumor growth of colorectal cancer cells. *Cancer Res*. 2014;74:775-786.
17. Wu J, Chai H, Xu X, Yu J, Gu Y. Histone methyltransferase SETD1A interacts with HIF1alpha to enhance glycolysis and promote cancer progression in gastric cancer. *Mol Oncol*. 2020;14:1397-1409.
18. Kang JY, Park JW, Hwang Y, et al. The H3K4 methyltransferase SETD1A is required for proliferation of non-small cell lung cancer cells by promoting S-phase progression. *Biochem Biophys Res Commun*. 2021;561:120-127.
19. Wu J, Chai H, Shan H, et al. Histone methyltransferase SETD1A induces epithelial-mesenchymal transition to promote invasion and metastasis through epigenetic reprogramming of snail in gastric cancer. *Front Cell Dev Biol*. 2021;9:657888.
20. Fang L, Teng H, Wang Y, et al. SET1A-mediated mono-methylation at K342 regulates YAP activation by blocking its nuclear export and promotes tumorigenesis. *Cancer Cell*. 2018;34:103-118.e109.
21. Wu ZH, Huang HM, Yang DL. Integrated analysis of the functions and prognostic values of RNA binding proteins in hepatocellular carcinoma. *BMC Gastroenterol*. 2021;21:265.
22. Ouyang H, Mou L, Luk C, et al. Immortal human pancreatic duct epithelial cell lines with near normal genotype and phenotype. *Am J Pathol*. 2000;157:1623-1631.
23. Assimon VA, Tang Y, Vargas JD, et al. CB-6644 is a selective inhibitor of the RUVBL1/2 complex with anticancer activity. *ACS Chem Biol*. 2019;14:236-244.
24. Salz T, Deng C, Pampo C, et al. Histone methyltransferase hSETD1A is a novel regulator of metastasis in breast cancer. *Mol Cancer Res*. 2015;13:461-469.
25. Okuno K, Akiyama Y, Shimada S, et al. Asymmetric dimethylation at histone H3 arginine 2 by PRMT6 in gastric cancer progression. *Carcinogenesis*. 2019;40:15-26.
26. Wagner K, Schulz P, Scholz A, Wiedenmann B, Menrad A. The targeted immunocytokine L19-IL2 efficiently inhibits the growth of orthotopic pancreatic cancer. *Clin Cancer Res*. 2008;14:4951-4960.
27. Zhu Y, Bai K, Yu J, Guo M. Association between histone methyltransferase hSETD1A and prognosis in patients with triple-negative breast cancer after surgery: a retrospective study in the Chinese female population. *Medicine (Baltimore)*. 2016;95:e3783.
28. Wang R, Liu J, Li K, et al. An SETD1A/Wnt/β-catenin feedback loop promotes NSCLC development. *J Exp Clin Cancer Res*. 2021;40:318.
29. Guo X, Li H, Zhang M, Li R. LncRNA GAS6 antisense RNA 1 facilitates the tumorigenesis of clear cell renal cell carcinoma by regulating the AMP-activated protein kinase/mTOR signaling pathway. *Oncol Lett*. 2021;22:727.

30. Kuppers DA, Arora S, Lim Y, et al. N(6)-methyladenosine mRNA marking promotes selective translation of regulons required for human erythropoiesis. *Nat Commun*. 2019;10:4596.
31. Tate CM, Lee JH, Skalnik DG. CXXC finger protein 1 restricts the Setd1A histone H3K4 methyltransferase complex to euchromatin. *FEBS J*. 2010;277:210-223.
32. Taniuchi K, Furihata M, Iwasaki S, et al. RUVBL1 Directly binds Actin filaments and induces formation of cell protrusions to promote pancreatic cancer cell invasion. *Int J Oncol*. 2014;44:1945-1954.
33. Ferbus D, Bovin C, Validire P, Goubin G. The zinc finger protein OZF (ZNF146) is overexpressed in colorectal cancer. *J Pathol*. 2003;200:177-182.
34. Mathsyaraja H, Catchpole J, Freie B, et al. Loss of MGA repression mediated by an atypical polycomb complex promotes tumor progression and invasiveness. *Elife*. 2021;10:e64212.
35. Alečković M, Wei Y, LeRoy G, et al. Identification of nidogen 1 as a lung metastasis protein through secretome analysis. *Genes Dev*. 2017;31:1439-1455.
36. Schneider J, Wood A, Lee JS, et al. Molecular regulation of histone H3 trimethylation by COMPASS and the regulation of gene expression. *Mol Cell*. 2005;19:849-856.
37. Yang L, Jin M, Park SJ, Seo SY, Jeong KW. SETD1A promotes proliferation of castration-resistant prostate cancer cells via FOXM1 transcription. *Cancers (Basel)*. 2020;12:1736.
38. Jin ML, Kim YW, Jin HL, et al. Aberrant expression of SETD1A promotes survival and migration of estrogen receptor α-positive breast cancer cells. *Int J Cancer*. 2018;143:2871-2883.
39. Baron BW, Baron RM, Baron JM. The relationship between RUVBL1 (pontin, TIP49, NMP238) and BCL6 in benign and malignant human lymphoid tissues. *Biochem Biophys Rep*. 2016;6:1-8.
40. Chen J, Liu G, Wu Y, et al. CircMYO10 promotes osteosarcoma progression by regulating miR-370-3p/RUVBL1 axis to enhance the transcriptional activity of beta-catenin/LEF1 complex via effects on chromatin remodeling. *Mol Cancer*. 2019;18:150.
41. Li H, Tong X, Xu Y, et al. Functional genetic variants of RUVBL1 predict overall survival of Chinese patients with epithelial ovarian cancer. *Carcinogenesis*. 2019;40:1209-1219.
42. Haurie V, Ménard L, Nicou A, et al. Adenosine triphosphatase pontin is overexpressed in hepatocellular carcinoma and coregulated with reptin through a new posttranslational mechanism. *Hepatology*. 2009;50:1871-1883.
43. Mao YQ, Houry WA. The pole of pontin and Reptin in cellular physiology and cancer etiology. *Front Mol Biosci*. 2017;4:58.
44. Grigoletto A, Lestienne P, Rosenbaum J. The multifaceted proteins Reptin and pontin as major players in cancer. *Biochim Biophys Acta*. 2011;1815:147-157.
45. Fan W, Xie J, Xia J, et al. RUVBL1-ITFG1 interaction is required for collective invasion in breast cancer. *Biochim Biophys Acta Gen Subj*. 2017;1861:1788-1800.
46. Vedadi M, Blazer L, Eram MS, Barsyte-Lovejoy D, Arrowsmith CH, Hajian T. Targeting human SET1/MLL family of proteins. *Protein Sci*. 2017;26:662-676.
47. Chen J, Feng J, Fang Z, et al. Anlotinib suppresses MLL-rearranged acute myeloid leukemia cell growth by inhibiting SETD1A/AKT-mediated DNA damage response. *Am J Transl Res*. 2021;13:1494-1504.

SUPPORTING INFORMATION

Additional supporting information can be found online in the Supporting Information section at the end of this article.

How to cite this article: Ishii T, Akiyama Y, Shimada S, et al. Identification of a novel target of SETD1A histone methyltransferase and the clinical significance in pancreatic cancer. *Cancer Sci*. 2023;114:463-476. doi: 10.1111/cas.15615